Work Summary

Further result for modifying the fidelity expression. Compared the target and pulse-driven evolution's properties.

Main Work

1. Explicit comparison of unitary evolution matrix
2. Example optimized pulses
3. Further examination on J-χ ratio
4. Pulse driven dynamics
5. Nearest neighbor interaction in tight-binding model
6. Lie-Trotter expansion

1 Explicit comparison of unitary evolution matrix

Last time, I showed an explicit comparison of the absolute values for the 6×6 unitary between the hopping levels. Here, just to further confirm the simulation, gives an explicit comparison of the imaginary and real values separately. Let evolution time to be $\tau = 2.0\mu$s, assume the target unitary is U_{targ}, then

$$Re(U_{targ}) = \begin{pmatrix} 0.5937 & 0. & 0. & 0. & 0. & 0.4063 \\ 0. & 0.5937 & 0. & 0. & -0.4063 & 0. \\ 0. & 0. & 0.1874 & 0. & 0. & 0. \\ 0. & 0. & 0. & 0.1874 & 0. & 0. \\ 0. & -0.4063 & 0. & 0. & 0.5937 & 0. \\ 0.4063 & 0. & 0. & 0. & 0. & 0.5937 \end{pmatrix}$$

and

$$Im(U_{targ}) = \begin{pmatrix} 0. & 0. & 0.4911 & -0.4911 & 0. & 0. \\ 0. & 0. & 0.4911 & 0.4911 & 0. & 0. \\ 0.4911 & 0.4911 & 0. & 0. & 0.4911 & -0.4911 \\ -0.4911 & 0.4911 & 0. & 0. & 0.4911 & 0.4911 \\ 0. & 0. & 0.4911 & 0.4911 & 0. & 0. \\ 0. & 0. & -0.4911 & 0.4911 & 0. & 0. \end{pmatrix}.$$

On the other hand, setting the max iterations for GRAPE to be 4000, the optimized final unitary has a ground-hop fidelity of 99.995%. The corresponding real and imaginary parts are

$$Re(U_{evol}) = \begin{pmatrix} -0.5761 & -0.0001 & 0.1184 & -0.1185 & 0.0009 & -0.3937 \\ 0. & -0.5759 & 0.1186 & 0.1185 & 0.3946 & 0.0001 \\ 0.119 & 0.1185 & -0.1819 & -0.0001 & 0.1186 & -0.119 \\ -0.1181 & 0.118 & 0.0002 & -0.1817 & 0.1182 & 0.1183 \\ -0.0006 & 0.3938 & 0.1188 & 0.1187 & -0.5762 & -0.0001 \\ -0.3949 & 0. & -0.1185 & 0.1184 & 0.0002 & -0.576 \end{pmatrix}$$

and

$$Im(U_{evol}) = \begin{pmatrix} -0.1435 & -0.0001 & -0.4767 & 0.477 & -0. & -0.0978 \\ 0. & -0.1431 & -0.4763 & -0.4767 & 0.0985 & 0.0005 \\ -0.4767 & -0.4766 & -0.045 & -0.0002 & -0.4759 & 0.4769 \\ 0.4758 & -0.4773 & -0.0002 & -0.0453 & -0.4769 & -0.4769 \\ -0.0005 & 0.0982 & -0.4768 & -0.4764 & -0.1437 & -0. \\ -0.0982 & 0.0004 & 0.4765 & -0.4764 & -0. & -0.1434 \end{pmatrix}.$$

Since the fidelity ignores global phases, this difference is understandable. To prove that, it can be shown that

$$|U_{targ}^{-1} U_{evol}| = \begin{pmatrix} 0.9999 & 0.0003 & 0.0002 & 0.0004 & 0.0012 & 0.0007 \\ 0.0003 & 0.9999 & 0.0002 & 0.0003 & 0.0007 & 0.0006 \\ 0.0002 & 0.0002 & 0.9999 & 0.0003 & 0.0003 & 0.0004 \\ 0.0005 & 0.0003 & 0.0002 & 1. & 0.0002 & 0.0002 \\ 0.0011 & 0.0007 & 0.0003 & 0.0002 & 1. & 0.0002 \\ 0.0007 & 0.0006 & 0.0004 & 0.0002 & 0.0002 & 1. \end{pmatrix}$$

with a global phase of around 0.244rad. Beside that, the optimized evolution unitary is decently close to the target unitary.

2 Example optimized pulses

The initial pulses are generally set to random pulses that are piece wise constant. The GRAPE-optimized pulses are usually much less random that the starting points. Just to give an example, set the evolution time to 5μs and optimize for around 1000 iterations, i.e. around 20 minutes. The resulting ground-hop fidelity is 99.9993%. The initial and final (optimized) pulses are shown in Figure 1.

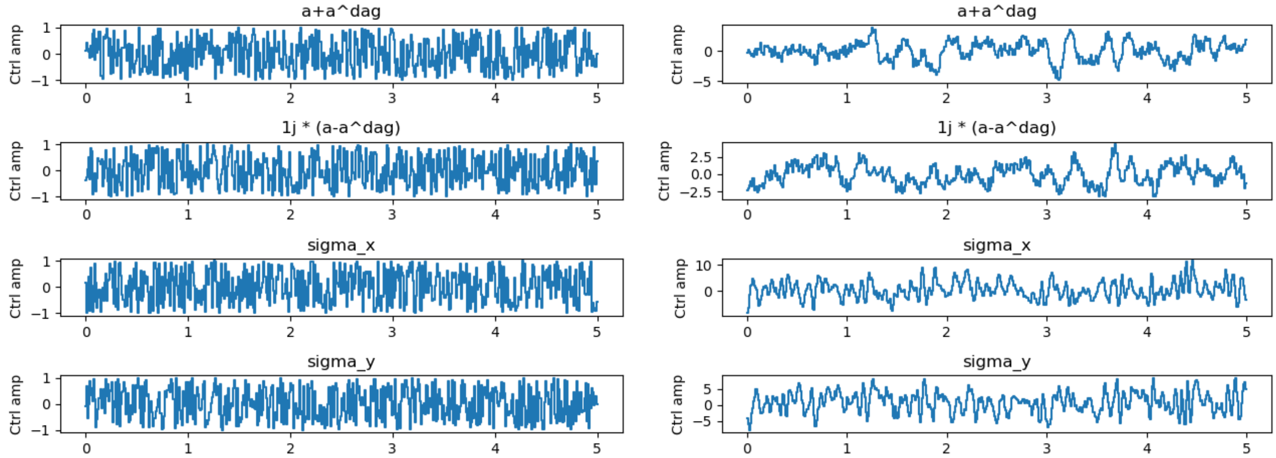

(a) Initial pulse shapes input to GRAPE algorithm

(b) Final optimized pulse shapes from GRAPE algorithm

Figure 1: Initial and final pulses.

3 Further examination on J-χ ratio

Similar to what's stated in the previous report, with JT product fixed, the ratio of J and χ can be translated to the ratio of T and T_{int}.

Last time, it is shown that the fidelity decreases with T increases since that means the system has more time to practice controls as shown in Figure 2.

In this section, it is aimed to show if the 'peak' at low T is because of a lack of iterations or because the system isn't capable enough. Focusing in the range from T=0.5T to T=1.5T, which is where the peak is at and also where it is more interesting and practical to avoid too much decoherence. Three Figures of different number of iterations are shown in Figure 3, 4, and 5.

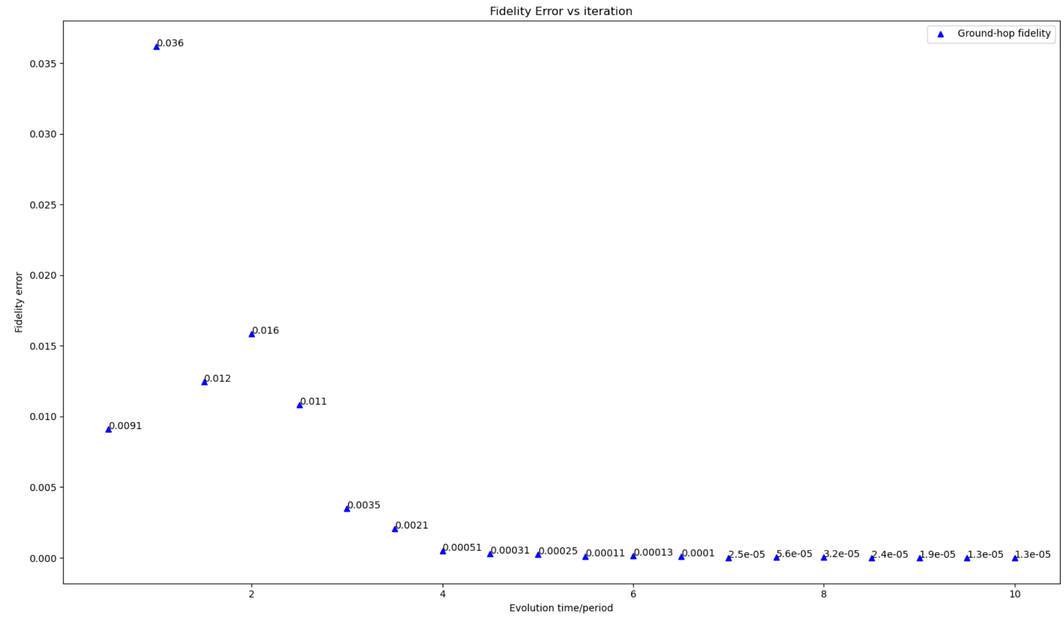

Figure 2: Fidelity error vs $n = T/T_{int}$. Fidelity calculation in algorithm using f_2. Only showing values of f_2.

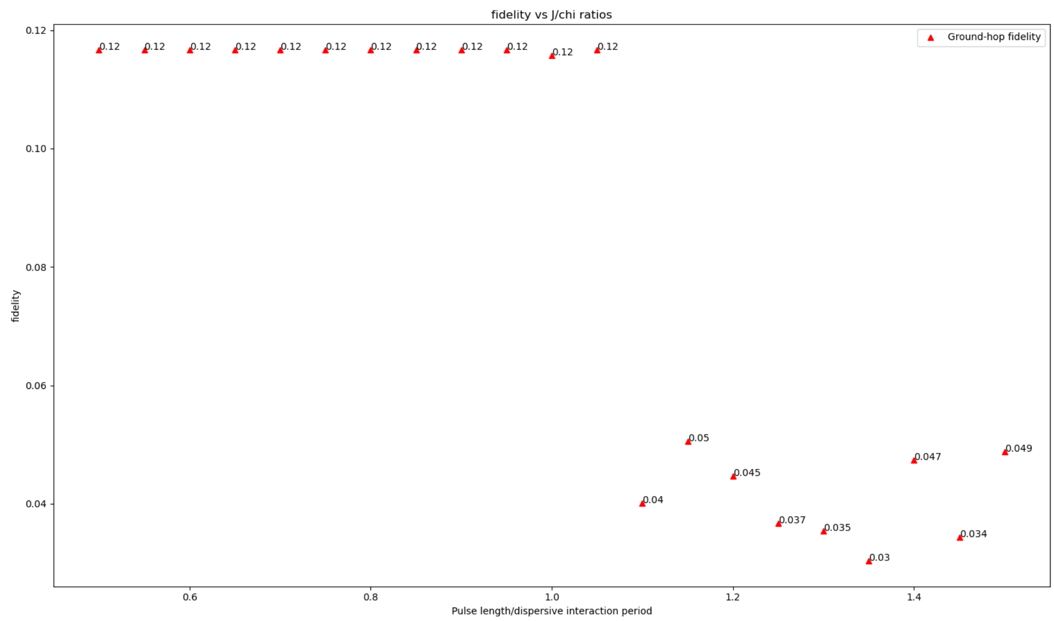

Figure 3: Fidelity error vs $n = T/T_{int}$. 500 iterations.

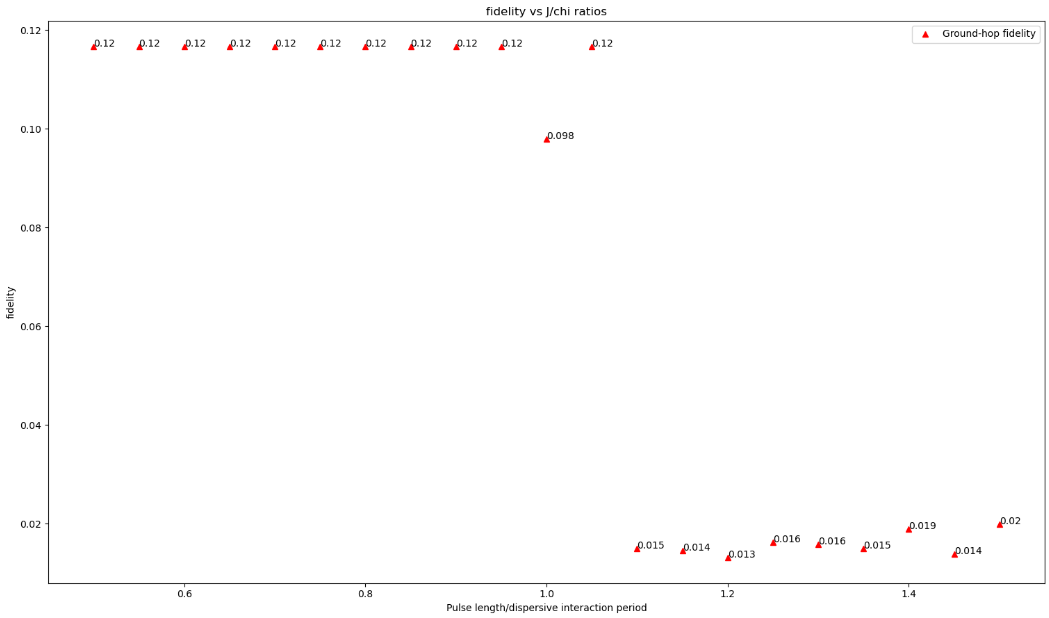

Figure 4: Fidelity error vs $n = T/T_{int}$. 1500 iterations.

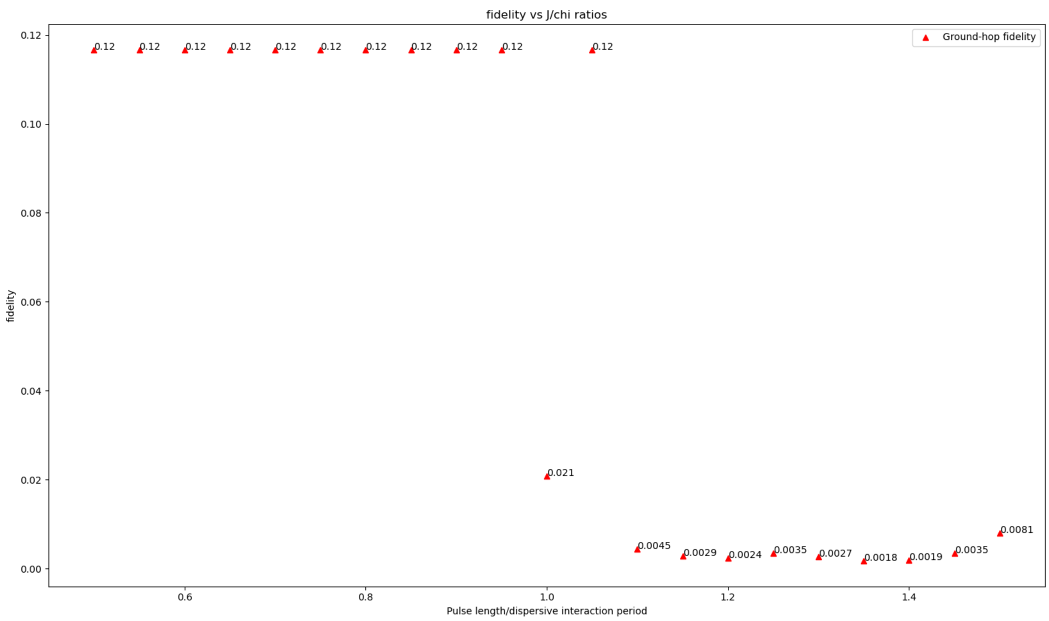

Figure 5: Fidelity error vs $n = T/T_{int}$. 10000 iterations.

4 Pulse driven dynamics

An example of the target evolution can be expressed in Figure 6. Here, the states start in energy level $|0\rangle$ in the cavity and evolve for $10\mu s$. There is certainly periodic behavior shown.

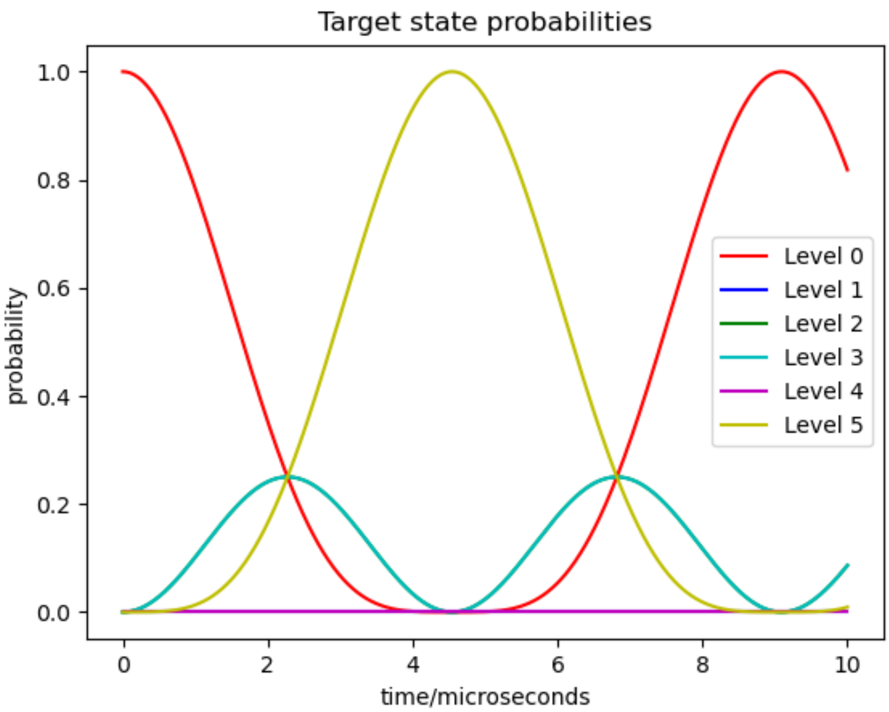

Figure 6: Target evolution of the first 6 energy level's probability density. Note that levels 2,3 and 1,4 have identical probabilities at any time because of symmetry.

Optimize the pulse sequence with a pulse length of $2\mu s$ in GRAPE. Drive the system numerically using the optimized pulse sequence repeatedly. In this case, to reach the $10\mu s$ time, the pulse sequence is applied 5 times. The comparison of state probabilities for the 6 states between target and pulse-driven evolution are shown in Figure 7.

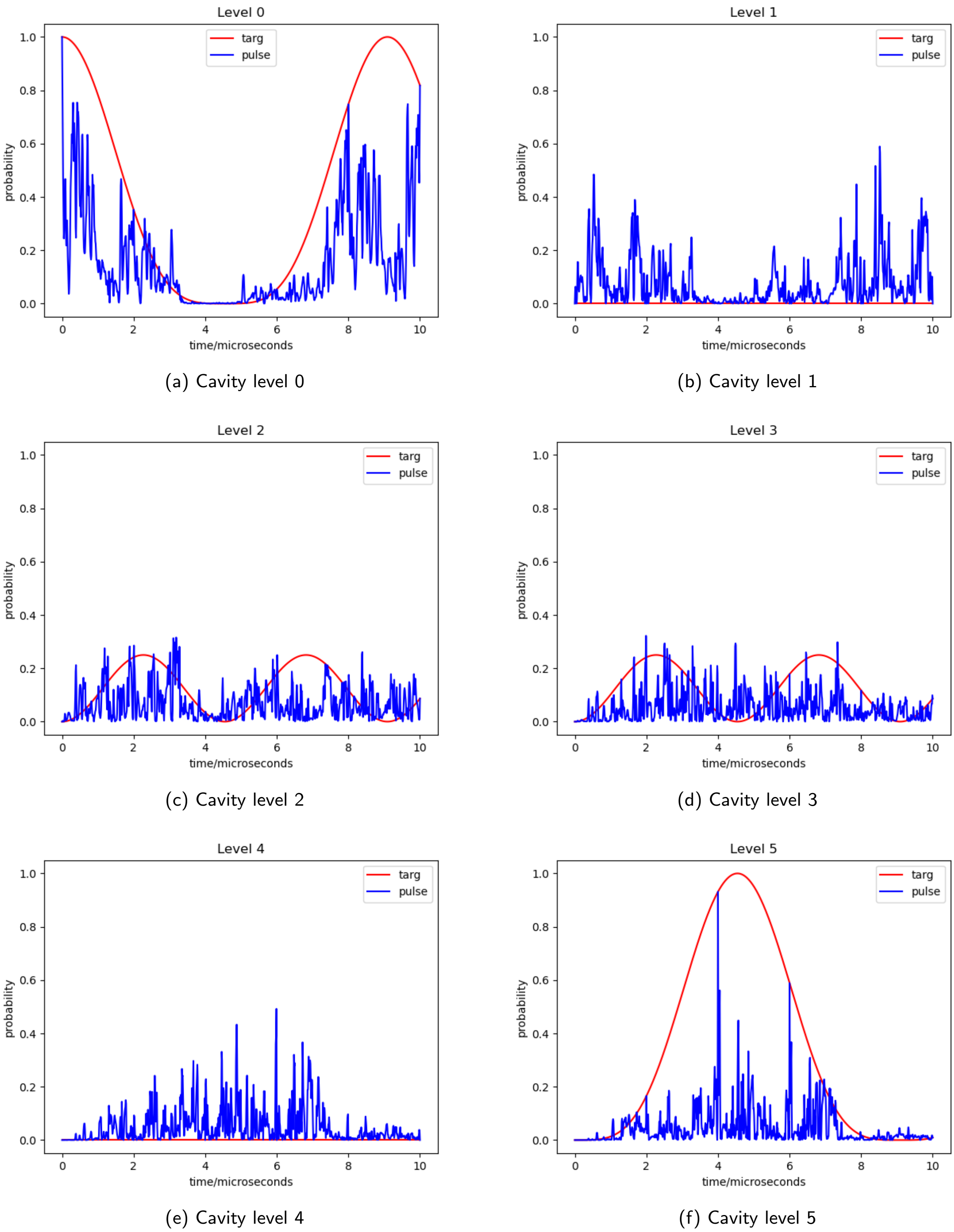

(a) Cavity level 0

(b) Cavity level 1

(c) Cavity level 2

(d) Cavity level 3

(e) Cavity level 4

(f) Cavity level 5

Figure 7: Comparing resulting probability for the first 6 energy levels from target and pulse-driven evolution.

4.1 Mapping back to the tight-binding model

The current mapping of basis is from the electron occupation states $\begin{pmatrix} |21\rangle \\ |41\rangle \\ |31\rangle \\ |42\rangle \\ |32\rangle \\ |43\rangle \end{pmatrix}$ to cavity energy levels $\begin{pmatrix} |0\rangle \\ |1\rangle \\ |2\rangle \\ |3\rangle \\ |4\rangle \\ |5\rangle \end{pmatrix}$. Therefore, mapping back to the tight-binding model gives the expected electron density giving the probability densities of the cavity levels. As a result, the comparison of electron densities from the target and pulse-driven evolution is shown in Figure 8.

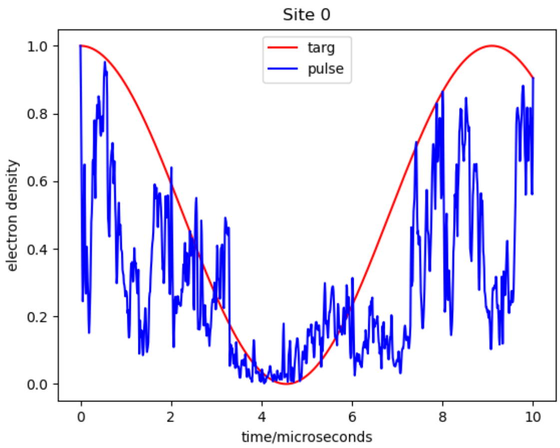

(a) Site 0

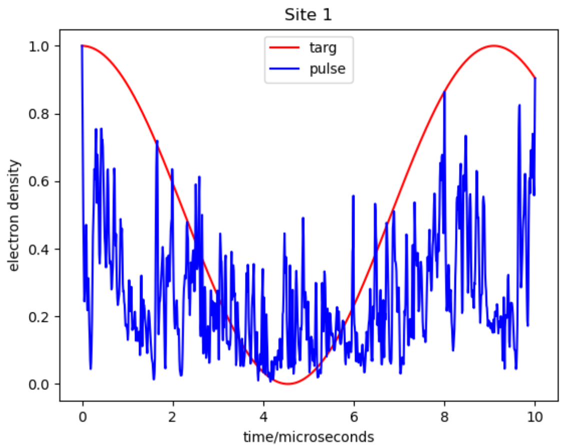

(b) Site 1

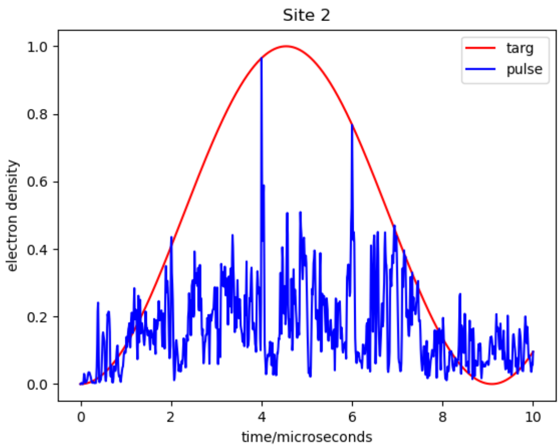

(c) Site 2

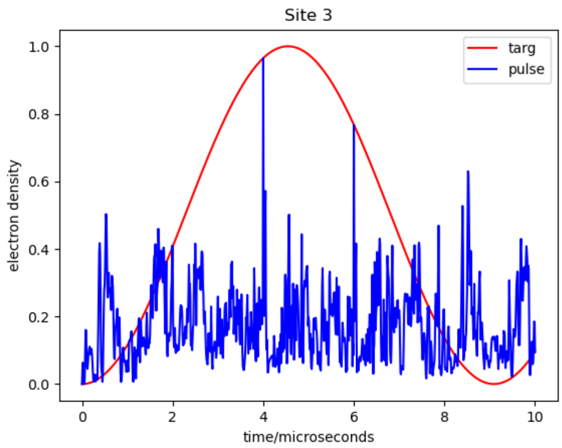

(d) Site 3

Figure 8: Comparing resulting electron densities for the 4 sites from target and pulse-driven evolution.

4.2 Infidelity measurement

I have thought about the ways to measure the infidelity or loss. The expected infidelity should go up as the number of pulse sequences applied increases. One that I used is the loss of electron densities, i.e. the difference in total electron density between the target and pulse-driven evolution. The electron density should conserve in the target evolution, which gives 2 electrons in this case. However, this measure can't take into account of the individual site's electron densities, so I am still thinking about how to improve it.

A plot of the electron density loss is shown in Figure 9. Here, the range of number of pulse sequences is extended to 100 pulse sequences. Note it is approximately linear.

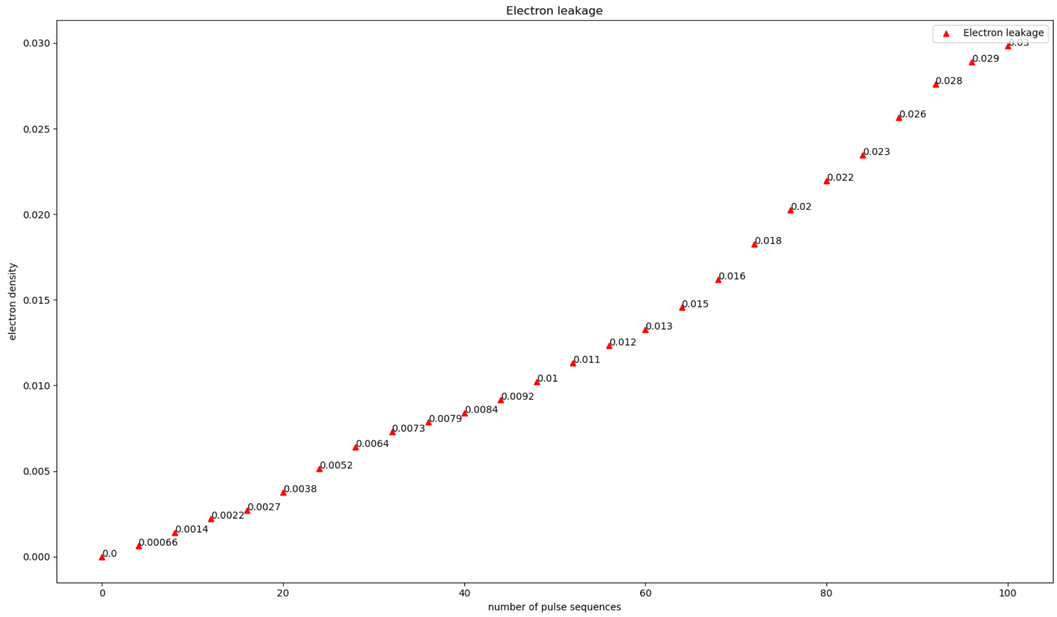

Figure 9: Electron density loss vs number of pulse sequence applied.

5 Nearest neighbor interaction in tight-binding model

In the tight-binding model, if the nearest neighbor interaction is included, then there will be positive energy when the electrons sit on two neighboring sites. Therefore, the resulting Hamiltonian in the cavity basis is shown in Equation 1.

$$\hat{H}_{neighbor} = K \begin{pmatrix} 1 & 0 & 0 & 0 & 0 & 0 \\ 0 & 1 & 0 & 0 & 0 & 0 \\ 0 & 0 & 0 & 0 & 0 & 0 \\ 0 & 0 & 0 & 0 & 0 & 0 \\ 0 & 0 & 0 & 0 & 1 & 0 \\ 0 & 0 & 0 & 0 & 0 & 1 \end{pmatrix} \tag{1}$$

6 Lie-Trotter expansion

The Lie-Trotter expansion can be a good approximation for separating exponentials with non-commutable operators. A second order formula is given as

$$e^{-i(\hat{H}_{hop}+\hat{H}_{neighbor})T} = \left(e^{-i\hat{H}_{hop}\frac{T}{2n}}e^{-i\hat{H}_{neighbor}\frac{T}{n}}e^{-i\hat{H}_{hop}\frac{T}{2n}}\right)^n + \mathcal{O}((JT)^3/n^2).$$

Here I have used the assumption that $J > K$.